

FEDOPENMATCH: TOWARDS SEMI-SUPERVISED FEDERATED LEARNING IN OPEN-SET ENVIRONMENTS

Anonymous authors

Paper under double-blind review

ABSTRACT

Semi-supervised federated learning (SSFL) has emerged as an effective approach to leverage unlabeled data distributed across multiple data owners for improving model generalization. Existing SSFL methods typically assume that labeled and unlabeled data share the same label space. However, in realistic federated scenarios, unlabeled data often contain categories absent from the labeled set, i.e., outliers, which can severely degrade the performance of SSFL algorithms. In this paper, we address this under-explored issue, formally propose the open-set semi-supervised federated learning (OSSFL) problem, and develop the first OSSFL framework, FedOpenMatch. Our method adopts a one-vs-all (OVA) classifier as the outlier detector, equipped with logit adjustment to mitigate inlier-outlier imbalance and a gradient stop mechanism to reduce feature interference between the OVA and inlier classifiers. In addition, we introduce the logit consistency regularization loss, yielding more robust performance. Extensive experiments on standard benchmarks across diverse data settings demonstrate the effectiveness of FedOpenMatch, which significantly outperforms the baselines.

1 INTRODUCTION

Federated learning (FL) allows multiple clients to collaboratively train models without sharing private data (McMahan et al., 2017; Kairouz et al., 2021). The privacy preserving nature has driven its wide applications in various fields, such as medicine (Sheller et al., 2020) and autonomous driving (Eid Kishawy et al., 2024). However, typical FL assumes that all distributed training samples are fully labeled, which is impractical in most cases as it requires that all clients have enough expertise knowledge, time and willingness to label their data.

Recently, *semi-supervised federated learning* (SSFL) has emerged as an effective solution to exploit the distributed unlabeled data with accessing to a limited number of labeled samples (Jeong et al., 2021). SSFL generates pseudo-labels for unlabeled data and then involves them into training. SSFL works can be approximately categorized into two types, *label-at-client* (Liu et al., 2024; Bai et al., 2024) and *label-at-server* (Diao et al., 2022; Lee et al., 2024), with respect to the location of labeled data. This work focuses on the latter setting, which is considered more practical as it does not assume clients have labeling capabilities. Instead, the server (e.g., autonomous driving company) often has plenty resources, and can afford to acquire a small number of labeled samples at a reasonable cost.

While previous works have made great progress in utilizing the unlabeled data, they all assume that unlabeled data share the same category set with labeled data. However, as the clients collect training samples independently and privately, it is inevitable for them to contain samples from unseen classes, i.e., outliers, so as the testing data. Standard SSFL algorithms do not have the ability to detect outliers and they will assign wrong pseudo-labels for outliers, which has been proven to hurt the model performance (Oliver et al., 2018). Moreover, outliers will be wrongly predicted as seen classes at inference stage, causing inevitable failures in critical application scenarios. Thus, it is critical to take the existence of outliers into consideration when designing SSFL algorithms.

On the other hand, there is a related research field called *open-set semi-supervised learning* (OSSL) (Saito et al., 2021), which is for centralized scenarios, where the model can access both labeled and unlabeled data simultaneously, and the unlabeled data contain samples of unseen classes. While federated settings pose additional challenges: the strict separation of labeled and unlabeled data makes client difficult to obtain correct supervision, and client training can be easily misled

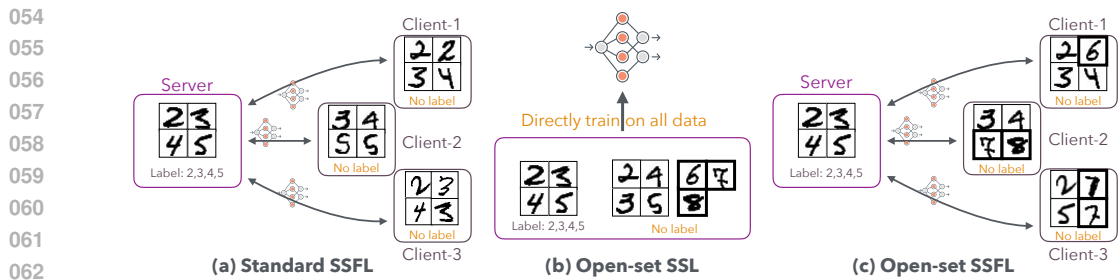


Figure 1: Illustration of the differences among (a) standard SSFL where all data are in the same category space ('2', '3', '4', '5'), (b) open-set SSL (OSSL) where the unlabeled data contain samples of unseen classes ('6', '7', '8'), and (c) our open-set SSFL (OSSFL) where unlabeled data in the clients have samples of classes ('6', '7', '8') different from that of the labeled data in the server.

by noisy pseudo-labels. Moreover, data heterogeneity across clients further exacerbates this issue. Therefore, naively adapting those OSSL algorithms into the federated learning setting will suffer severe performance degradation, as detailed in Sec. 4.2.

To address the problem caused by outliers in SSFL, in this paper we first formulate a new problem called Open-set Semi-supervised Federated Learning (OSSFL in short), in other words, OSSL in FL. Fig. 1 illustrates the differences among SSFL, OSSL and our OSSFL. Concretely, SSFL is SSL in FL setting; OSSL is SSL in centralized open-set scenarios; and our OSSFL is SSL in federated open-set scenarios. To the best of our knowledge, up to now there has been no OSSFL work in the literature. Then, we design the first OSSFL framework, **FedOpenMatch**. Specifically, we employ an *one-vs-all* (OVA) classifier serving as the outlier detector to help generate high-quality inlier pseudo-labels during training. We also introduce gradient stop to address the interference issue between inlier and OVA classifier, and employ logit adjustment for combating the imbalanced OVA prediction, avoiding the inliers being recognized as outliers and discarded during training. To further exploit the unlabeled samples including both unconfident inliers and outliers, we devise a logit consistency regularization loss by modifying the early proposed probability consistency regularization loss (Saito et al., 2021), which significantly improves the performance. Comprehensive experiments on three commonly used benchmarks under various data settings show that FedOpenMatch can significantly boost the open-set accuracy up to 14.33% on the CIFAR-100 dataset.

In summary, the contributions of this paper are as follows: 1) We formally propose the new problem: open-set semi-supervised federated learning (OSSFL), to tackle the outlier issue in SSFL, i.e., to extend OSSL to FL scenarios. 2) We develop a simple but powerful OSSFL framework, FedOpenMatch, which consists of three components: gradient stop, logit adjustment, and logit consistency regularization. 3) For comprehensive performance evaluation and comparison, we implement several OSSFL baselines by adapting the latest OSSL algorithms to the OSSFL setting. 4) We conduct extensive experiments to evaluate FedOpenMatch, which show that FedOpenMatch significantly outperforms the baselines on commonly used benchmarks across diverse data settings.

2 RELATED WORK

Semi-supervised Learning (SSL). SSL is a learning paradigm that leverages both labeled and unlabeled data. Early advances in SSL were largely driven by two techniques: consistency regularization (Xie et al., 2020; Miyato et al., 2018) and pseudo-labeling (Lee et al., 2013). More recently, FixMatch (Sohn et al., 2020) integrates both strategies into a simple yet highly effective framework, achieving high performance across a variety of benchmarks. Building on this foundation, subsequent works have introduced further refinements. For example, FlexMatch (Zhang et al., 2021), FreeMatch (Wang et al., 2022), InstanT (Li et al., 2023a), and Park et al. (2025) adopt fine-grained thresholding mechanisms to generate high-quality pseudo-labels. SoftMatch (Chen et al., 2023) proposes a sample re-weighting strategy, while DST (Chen et al., 2022) and FlatMatch (Huang et al., 2023) enhance robustness against noisy pseudo-labels. Despite their success, all of these methods share a fundamental limitation: they assume that labeled and unlabeled data are drawn from the same category set, which rarely holds in real-world scenarios.

108

109 Table 1: A qualitative comparison among SSFL, OSSL, FOSR, and OSSFL from four perspectives.

110

	Distributed	Scarce labels	Open-set unlabeled training	Open-set testing
FOSR	✓	✗	✗	✓
SSFL	✓	✓	✗	✗
OSSL	✗	✓	✓	✓
OSSFL	✓	✓	✓	✓

111

112

Open-set SSL. This line of research extends conventional SSL to scenarios where unlabeled data may contain samples from unseen classes. Early OSSL methods typically follow a *detect-and-filter* paradigm, aiming to reduce the negative impact of outliers by detecting and discarding them. Different approaches have been explored for outlier detection, including ensemble confidence (Chen et al., 2020), energy-based scoring function (He et al., 2022), binary classification (Yu et al., 2020), weighting function (Guo et al., 2020), and cross-modal matching (Huang et al., 2021). More recent methods achieve higher performance by employing *one-vs-all* (*OVA*) classifiers as outlier detectors (Saito et al., 2021; Li et al., 2023b; Fan et al., 2023; Hang & Zhang, 2024), along with auxiliary strategies such as probability consistency regularization (Saito et al., 2021) and negative pseudo-label mining (Fan et al., 2023; Hang & Zhang, 2024). To reduce the dependence on a reliable OVA classifier, IOMatch (Li et al., 2023b) reformulates OSSL into a $(K + 1)$ -way classification problem by grouping all unseen categories into a single “unknown” class. In contrast, BDMatch (Hang & Zhang, 2024) redefines OSSL as multiple binary SSL tasks, thereby unifying the pseudo-labeling space for both seen and unseen samples.

130

131

Semi-supervised Federated Learning. Existing SSFL works can be broadly categorized into two paradigms: *label-at-client*, where each client has access to both labeled and unlabeled samples (Liang et al., 2022; Zhang et al., 2023a;b; Bai et al., 2024; Liu et al., 2024; Zhang et al., 2024; Liao et al., 2025); and *label-at-server*, where clients hold only unlabeled data while the server maintains a small labeled dataset (Jeong et al., 2021; Diao et al., 2022; Kim et al., 2023; Yang et al., 2024; Lee et al., 2024). This work focuses on the *label-at-server* setting, which is considered more realistic in practice. A key challenge in SSFL is the generation of reliable pseudo-labels to maximize the utility of distributed unlabeled data. Several strategies have been proposed. FedMatch (Jeong et al., 2021) adopts disjoint learning to reduce interference between labeled and unlabeled knowledge. SemiFL (Diao et al., 2022) mitigates pseudo-label degradation by generating pseudo-labels with global model instead of local ones. FL^2 (Lee et al., 2024) introduces sharpness-aware consistency regularization and adaptive thresholding, enabling more effective exploitation of unlabeled data. Kim et al. (2023) and Yang et al. (2024) focus on different tasks.

143

144

Federated Open-set Recognition (FOSR). FOSR (Yang et al., 2023; Zhu et al., 2023) has the same goal to accurately classify samples from seen classes while detecting outliers from unseen classes, but differs in the training process. FOSR trains models with completely labeled samples from seen classes while OSSFL trains with unlabeled open-set dataset. This distinction makes OSSFL more challenging, as it must tackle the difficulties of semi-supervised learning and open-set recognition.

145

146

147

148

149

150

151

152

153

154

155

156

157

158

159

160

161

3 THE FEDOPENMATCH METHOD

3.1 PROBLEM DEFINITION AND FRAMEWORK

Problem definition. We assume there are a central *server* holds a small labeled dataset $D_s = \{x_{s;i}, y_{s;i}\}_{i=1}^{N_s}$ where $y_{s;i} \in Y = [1, \dots, K]$ is the label of sample $x_{s;i}$ and Y is the set of indexes

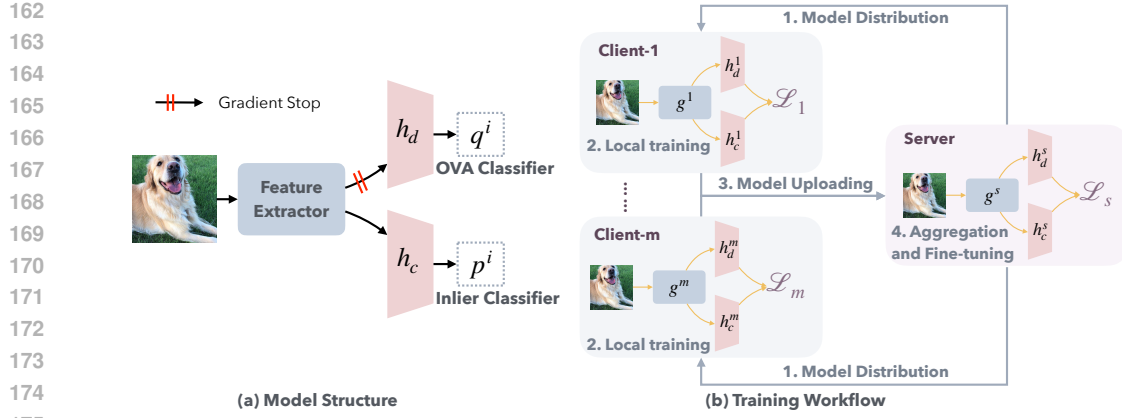


Figure 2: (a) The model architecture, consisting of a shared feature extractor, an inlier classifier, and an OVA classifier. (b) The training workflow. In each communication round, the server and clients alternatively update their models, which is abstracted into four stages: (1) model distribution, (2) client training, (3) model uploading, and (4) server aggregation and fine-tuning.

of K seen classes, and M clients, each of which has only an unlabeled dataset $D_u^m = \{x_{m;i}\}_{i=1}^{N_m}$. Typically, $\sum_{m=1}^M N_m \gg N_s$. In the open-set setting, the category of unlabeled sample $x_{m;i}$ is not guaranteed to be one of the K seen classes. The goal of OSSFL is to learn a model that can classify the unlabeled samples of seen classes (i.e., inliers) into correct seen classes while identifying the unlabeled samples of unseen classes (i.e., outliers).

Framework. FedOpenMatch is a multi-task learning framework that jointly trains an inlier classifier and an outlier detector. The whole model f consists of a shared feature extractor g , an inlier classifier h_c and an OVA classifier h_d . For the K -classification task, the inlier classifier outputs a K -dimensional logit $p : \{p^k\}_{k=1}^K = h_c \circ g(x)$. The OVA classifier is composed of K binary classifiers, each distinguishing the k -th target class from the remaining seen and unseen classes. For a sample x , it outputs $2K$ -dimensional logit $q : \{q^k : \{q_0^k, q_1^k\}\}_{k=1}^K = h_d \circ g(x)$, where q_0^k and q_1^k represent the score of x being an outlier or an inlier with respect to class k . For simplicity, we denote by \hat{p}_i and p_i the inlier predictions of $\alpha(x_i)$ and $\mathcal{A}(x_i)$ respectively. Here, $\alpha(\cdot)$ and $\mathcal{A}(\cdot)$ denote weak data augmentation (e.g., random cropping and flipping) and strong data augmentation (RandAugment (Cubuk et al., 2020)). Similarly, \hat{q}_i and q_i denote the OVA predictions.

In each communication round t , the server first trains the model by minimizing

$$\mathcal{L}_s = \frac{1}{N_s} \sum_{i=1}^{N_s} \ell_{ce}(p_i, y_i) + \ell_{ova}(q_i, y_i), \quad (1)$$

where ℓ_{ce} denotes the cross-entropy loss, and ℓ_{ova} is the loss of the OVA classifier where we adopt the hard-negative sub-classifier sampling technique (Saito et al., 2021), which is formulated as

$$\ell_{ova}(q_i, y_i) = -\log(q_{i;1}^y) - \min_{k \neq y} \log(q_{i;0}^k). \quad (2)$$

Once the server training is completed, the updated model is distributed to a subset of randomly-selected clients. Then, each selected client m updates the model by optimizing

$$\mathcal{L}_m = \mathcal{L}_m^{in} + \mathcal{L}_m^{ova} + \mathcal{L}_m^{lcr}, \quad (3)$$

where \mathcal{L}_m^{lcr} is the weak-strong logit consistency regularization defined in Eq. (8), \mathcal{L}_m^{in} is the loss of the inlier classifier with confident inlier pseudo-labels, and \mathcal{L}_m^{ova} is the loss of the OVA classifier. Specifically, \mathcal{L}_m^{in} and \mathcal{L}_m^{ova} are formulated as follows:

$$\mathcal{L}_m^{in} = \frac{1}{N_m} \sum_{i=1}^{N_m} (\mathbb{I}(\Gamma(\hat{p}_i) \geq \tau_{in}) \wedge \mathbb{I}(\hat{q}_{i;1}^{\hat{y}_i} \geq 0.5)) \ell_{ce}(p_i, \hat{y}_i), \quad (4)$$

$$\mathcal{L}_m^{ova} = \frac{1}{N_m} \sum_{i=1}^{N_m} \sum_{k=1}^K (\mathbb{I}(\hat{q}_{i;1}^k \geq \tau_{pos}) \vee \mathbb{I}(\hat{q}_{i;1}^k \leq \tau_{neg})) \ell_{bce}(q_i^k, \mathbb{I}(\hat{q}_{i;1}^k > \hat{q}_{i;0}^k)), \quad (5)$$

where $\hat{y}^i = \text{argmax}(\hat{p}^i)$ is the inlier pseudo-label, $\Gamma(\hat{p}_i) = \max \text{softmax}(\hat{p}_i)$ computes the confidence of inlier prediction, τ_{in} , τ_{pos} and τ_{neg} are predefined thresholds for inlier pseudo-labels, positive and negative OVA pseudo-labels respectively, and ℓ_{bce} is the binary cross-entropy loss. After local updates, the client models are aggregated to obtain the new global model $f = \sum_{m=1}^{\mu M} w_m \cdot f_m$, where $\{w_1, \dots, w_{\mu M}\}$ denotes the aggregation weights, and μ presents client join ratio.

To ensure pseudo-label stability during local training, we generate pseudo-labels using the global model at the beginning of each round and keep them fixed throughout the client updates. This prevents local training from being biased by noisy labels arising from the scarcity of supervision. Furthermore, we introduce a gradient stop strategy (Sec. 3.2) and a logit adjustment mechanism (Sec. 3.3) to further improve the performance.

3.2 STOP GRADIENT FOR DECOUPLED FEATURE SPACE

In our framework, the OVA classifier and the inlier classifier share the same feature extractor, but differ in optimization objectives. The inlier classifier pulls features toward their corresponding class centers while pushing them away from that of the other classes. In contrast, the OVA classifier seeks to separate each target class from the remaining classes. Consequently, the two branches inevitably interfere with each other in the shared feature space. Prior OSSL methods (Fan et al., 2023; Li et al., 2023b) have attempted to mitigate this issue by introducing projection layers to map features into task-specific spaces. However, the divergence in update directions persists, as evidenced by the low similarity between feature gradients of the two branches (see the results in Fig. 5 of Appendix A.2).

To address this challenge, we propose gradient stop (GS), blocking the gradient flow from the OVA branch to the shared feature extractor. The intuition is that the OVA classifier can effectively distinguish inliers from outliers using a feature space where intra-class compactness and inter-class separability are already enforced by the inlier classifier. Our ablation studies (Sec. 4.3) further validate the effectiveness of this gradient stop strategy.

3.3 LOGIT ADJUSTMENT FOR BALANCED OVA PREDICTION

During training, we observe that most unlabeled samples (including true inliers) are classified as outliers and thus discarded, leading to a low data utilization rate (see Fig. 9 in Appendix A.2). This phenomenon arises because the OVA classifier is inherently biased toward the majority class—outliers. Specifically, for each class k , all samples of the remaining $K-1$ classes serve as outliers during training. As K grows, the imbalance between inliers and outliers becomes more severe, which biases the binary classifiers toward predicting outliers, causing many true inliers to be mistakenly rejected.

To address this, we adopt a logit adjustment strategy inspired by Menon et al. (2021). Specifically, the logits for the OVA loss ℓ_{ova} defined in Eq. (2) are corrected as follows:

$$q^k = q^k + \omega \log \pi, \quad (6)$$

where $\pi = \{\frac{K-1}{K}, \frac{1}{K}\}$ represents the class prior probabilities of outliers and inliers, under the assumption of a balanced labeled dataset, and ω is a tunable scaling factor. This adjustment counteracts the imbalance by amplifying the contribution of inlier predictions, preventing them from being overwhelmed by the dominant outlier updates. We further validate the effectiveness of this logit adjustment in Sec. 4.3.

3.4 WEAK-STRONG LOGIT CONSISTENCY REGULARIZATION

In semi-supervised learning, effectively exploiting unlabeled samples is crucial for improving model performance. In Sec. 3.3, we introduce logit adjustment to ensure that as many inliers as possible are utilized. Nevertheless, a large portion of unlabeled data—including low-confidence inliers and outliers—still remain underexploited. Prior OSSL work (Saito et al., 2021) proposed the *soft open-set consistency regularization loss* (SOCR), defined as

$$\mathcal{L}^{oc} = \lambda \frac{1}{N_m} \sum_{i=1}^{N_m} mse(\text{softmax}(q_i), \text{softmax}(\hat{q}_i)) + mse(\text{softmax}(p_i), \text{softmax}(\hat{p}_i)), \quad (7)$$

where λ is a weighting factor. SOCR encourages the model to focus on label-related features by minimizing the divergence between predictions from two augmented views of the same sample.

Interestingly, we find that removing the softmax operation and directly enforcing consistency at the *logit* level yields better performance. We denote this as the *logit consistency regularization* (LCR):

$$\mathcal{L}_m^{lcr} = \lambda \frac{1}{N_m} \sum_{i=1}^{N_m} mse(q_i, \hat{q}_i) + mse(p_i, \hat{p}_i). \quad (8)$$

Ablation studies in Sec. 4.3 demonstrate that Eq. (8) significantly outperforms Eq. (7). We conjecture that logit-level regularization provides a stronger and more direct training signal by enforcing consistency between raw logits, whereas probability-level consistency (after softmax) primarily aligns distributions, which does not necessarily ensure consistent decision boundaries.

4 EVALUATION

4.1 EXPERIMENTAL SETUP

Datasets. Following prior studies, we evaluate FedOpenMatch on three widely used benchmarks: CIFAR-10, CIFAR-100 (Krizhevsky et al., 2009), and SVHN (Netzer et al., 2011). To simulate data heterogeneity across clients, we sample client data partitions from a Dirichlet distribution $Dir(\alpha)$, where smaller α corresponds to higher heterogeneity. In our experiments, we set $\alpha \in \{0.1, 0.3\}$. For each dataset, a subset of classes is designated as seen classes, and a small fraction of them are selected as labeled data. For brevity, we denote the data configuration as $D@X@Y@Z$ where D is the dataset name, X is the number of seen classes, Y is the number of labeled samples per class, and Z indicates the partition setting.

Baselines. To validate the effectiveness of FedOpenMatch, we compare it against three categories of approaches: (i) *labeled data only*, which serves as the lower bound; (ii) *standard SSFL* methods; and (iii) *open-set SSFL* methods. For standard SSFL methods, we include representative works with publicly available implementations: SemiFL (Diao et al., 2022), FedLabel (Cho et al., 2023), and FL^2 (Lee et al., 2024). We exclude FedMatch since prior work (Diao et al., 2022) consistently reports its performance to be inferior to the labeled-only baseline. To the best of our knowledge, FedOpenMatch is the first attempt to tackle the open-set SSFL problem. As there are no direct baselines in this setting, we adapt recent OSSFL methods originally designed for centralized training into the federated scenario, yielding federated counterparts of OpenMatch (Saito et al., 2021), SSB (Fan et al., 2023), IOMatch (Li et al., 2023b), and BDMatch (Hang & Zhang, 2024). Due to space limit, the implementation details are present in Appendix A.1.

Evaluation Metrics. Following prior work (Li et al., 2023b), we adopt two complementary metrics to assess performance: (i) **Closed-set accuracy** evaluates the ability of an OSSFL algorithm to leverage open-set unlabeled data in order to improve classification performance on the seen classes only. (ii) **Open-set accuracy** measures performance in the realistic open-set environment, where both seen and unseen classes coexist. To enable evaluation, we treat all unseen classes as a single additional category, yielding a total of $K + 1$ classes. We report *Balanced Accuracy* (BA) as:

$$BA = \frac{1}{K+1} \sum_{k=1}^{K+1} \text{Recall}^k,$$

where Recall^k denotes the recall for class k .

4.2 MAIN RESULTS

Results on CIFAR-100. Following prior works, we split CIFAR-100 according to super-classes. Experiments are conducted with either 80 or 50 seen classes, treating the remaining classes as unseen. For each seen class, 10 or 25 samples are selected as the labeled set. Tab. 2 and Tab. 3 preset the results of closed-set accuracy and open-set accuracy, respectively. Since standard SSFL algorithms cannot detect outliers, open-set accuracy is only compared among OSSFL approaches. FedOpenMatch consistently outperforms existing methods on both metrics. For example, under the CIFAR-100@80@25@Dir(0.1) setting, closed-set and open-set accuracy are improved by up to 7.11% and 14.33%, respectively, demonstrating the effectiveness of our approach.

324
325 Table 2: Results of **closed-set accuracy** on **CIFAR-100** across eight different data settings.
326
327

	#Labels per class	#Seen/Unseen classes		80/20		50/50	
		10		25		10	
		Partially		17.29±0.47	18.35±0.32	22.02±1.30	22.73±0.13
Dir(0.3)	SemiFL	NeurIPS'22	29.64±0.47	38.81±1.83	43.45±1.20	53.82±1.56	
	FedLabel	ICCV'23	35.76±0.99	47.81±0.74	47.84±0.47	58.71±0.23	
	<i>FL</i> ²	NeurIPS'24	35.08±0.01	45.23±0.01	46.10±0.79	53.95±0.84	
	OpenMatch	NeurIPS'21	22.25±2.63	34.58±1.59	32.93±1.05	28.68±16.9	
	SSB	ICCV'23	5.14±3.97	9.68±11.2	24.28±19.4	44.23±3.21	
	IOMatch	ICCV'23	37.59±1.29	47.50±1.09	48.35±1.49	56.44±1.23	
	BDMatch	ICML'24	34.05±0.98	42.19±1.33	46.57±2.27	37.45±25.9	
	FedOpenMatch	Ours	39.45±1.04	52.96±0.67	49.94±1.72	60.19±0.97	
	SemiFL	NeurIPS'22	28.62±1.41	35.93±1.15	39.56±2.04	48.00±0.75	
	FedLabel	ICCV'23	32.88±0.82	41.40±1.24	44.13±1.76	50.37±0.73	
Dir(0.1)	<i>FL</i> ²	NeurIPS'24	32.42±1.48	42.87±1.49	42.05±0.52	48.24±1.76	
	OpenMatch	NeurIPS'21	21.83±2.25	33.55±1.50	30.92±0.92	3.48±1.30	
	SSB	ICCV'23	8.93±2.93	9.30±13.9	36.14±1.65	30.55±19.6	
	IOMatch	ICCV'23	35.13±0.54	43.28±1.15	46.44±0.88	50.39±1.27	
	BDMatch	ICML'24	32.95±2.26	40.41±0.53	44.60±2.86	35.28±17.7	
	FedOpenMatch	Ours	37.11±0.18	50.39±0.35	46.66±0.14	56.54±0.82	

347
348 Table 3: Results of **open-set accuracy** on **CIFAR-100** across eight different data settings.
349

	#Labels per class	#Seen/Unseen		80/20		50/50	
		10		25		10	
		Partially		16.08±0.31	17.71±0.67	21.29±1.27	17.76±0.44
Dir(0.3)	OpenMatch	NeurIPS'21	2.11±0.77	1.74±0.33	1.97±0.01	1.99±0.04	
	SSB	ICCV'23	4.06±2.81	6.40±7.20	16.95±12.9	28.62±3.24	
	IOMatch	ICCV'23	28.66±0.85	37.72±2.06	42.86±0.83	49.45±1.92	
	BDMatch	ICML'24	23.19±1.86	29.38±2.53	39.15±3.39	31.14±25.4	
	FedOpenMatch	Ours	38.97±1.03	50.40±0.42	46.29±0.87	59.01±0.95	
	OpenMatch	NeurIPS'21	2.41±0.66	2.46±0.78	2.12±0.27	2.36±0.38	
	SSB	ICCV'23	6.31±1.95	6.09±8.42	22.08±1.00	20.19±12.2	
	IOMatch	ICCV'23	27.20±1.37	33.02±0.33	41.10±0.32	43.39±0.80	
	BDMatch	ICML'24	23.20±1.30	29.51±0.99	33.46±2.76	30.54±15.3	
	FedOpenMatch	Ours	36.65±2.43	47.35±2.98	43.91±0.65	54.60±1.53	

367 **Results on CIFAR-10 and SVHN.** For CIFAR-10, we follow prior studies (Li et al., 2023b) and
368 select the animal classes (6 classes) as seen classes. For SVHN, classes 2 through 7 are treated
369 as seen. For each seen class, 25 or 40 samples are randomly selected as the labeled set. Results
370 of closed-set and open-set accuracy are presented in Tab. 4 and Tab. 5, respectively. The results
371 highlight the improvements achieved by FedOpenMatch, particularly under highly heterogeneous
372 settings (Dir(0.1)).

373 **Summary.** The results above show that directly adapting OSSL algorithms to the federated setting
374 leads to unstable performance. For instance, SSB and OpenMatch often fail to surpass the lower-
375 bound baseline, despite sharing the same backbone architecture as our method. To investigate the
376 cause, we visualize the utilization rate and pseudo-label accuracy in Figs. 9 and 10 in Appendix A.2.
377 As illustrated, OpenMatch maintains a persistently low utilization rate of unlabeled data throughout
378 training. This is mainly due to its “detect-and-filter” strategy, where the imbalanced OVA classifier

Table 4: Results of **closed-set accuracy** on **CIFAR10** and **SVHN**.

Dataset-#Seen/Unseen classes		CIFAR10-6/4		SVHN-6/4	
		#Labels per class	40	25	40
	Partially		42.47±0.73	38.35±1.11	70.29±4.83
	SemiFL	NeurIPS'22	33.96±17.5	19.02±2.48	52.57±14.0
	FedLabel	ICCV'23	70.21±1.09	64.09±2.08	83.75±0.15
	<i>FL</i> ²	NeurIPS'24	55.69±1.33	53.39±2.79	77.93±1.42
	OpenMatch	NeurIPS'21	15.42±1.53	16.50±0.28	36.54±15.0
Dir(0.3)	SSB	ICCV'23	16.67±0.00	16.67±0.00	16.19±3.28
	IOMatch	ICCV'23	72.32±0.42	73.05±0.34	84.34±1.17
	BDMatch	ICML'24	53.16±27.8	43.29±19.7	82.12±2.01
	FedOpenMatch	Ours	73.32±1.12	72.45±1.26	84.86±1.57
	SemiFL	NeurIPS'22	28.50±16.7	17.26±0.83	70.03±4.41
Dir(0.1)	FedLabel	ICCV'23	59.36±0.59	54.22±1.93	77.67±2.64
	<i>FL</i> ²	NeurIPS'24	50.82±2.07	45.29±3.24	72.73±2.53
	OpenMatch	NeurIPS'21	16.68±0.16	16.63±0.04	63.66±12.3
	SSB	ICCV'23	16.67±0.00	16.67±0.00	12.41±0.00
	IOMatch	ICCV'23	64.79±1.55	59.60±0.39	79.48±0.43
	BDMatch	ICML'24	36.87±21.7	51.73±3.22	80.92±1.39
	FedOpenMatch	Ours	65.19±2.83	60.89±0.71	82.63±1.50
					78.36±0.74

Table 5: Results of **open-set accuracy** on **CIFAR10** and **SVHN**.

Dataset-#Seen/Unseen		CIFAR10-6/4		SVHN-6/4	
		#Labels per class	40	25	40
	Partially		36.02±0.66	32.32±0.75	60.44±4.59
	OpenMatch	NeurIPS'21	14.28±0.00	14.28±0.00	14.28±0.00
	SSB	ICCV'23	14.39±0.18	14.42±0.24	14.29±0.00
Dir(0.3)	IOMatch	ICCV'23	61.65±0.48	61.82±0.42	71.78±1.30
	BDMatch	ICML'24	42.62±24.5	24.59±17.8	69.36±1.48
	FedOpenMatch	Ours	62.26±0.51	61.98±2.18	71.87±0.83
	OpenMatch	NeurIPS'21	14.28±0.00	14.29±0.00	53.59±15.2
	SSB	ICCV'23	14.30±0.02	14.33±0.07	15.65±2.14
Dir(0.1)	IOMatch	ICCV'23	54.94±1.37	50.71±1.78	68.13±0.21
	BDMatch	ICML'24	25.86±20.1	24.65±17.9	67.49±1.18
	FedOpenMatch	Ours	55.27±2.21	51.45±0.45	70.57±0.93
					66.70±1.02

mistakenly identifies most samples as outliers, leaving a large portion of informative data underutilized. This observation highlights the necessity of our proposed logit adjustment. In contrast, SSB achieves higher utilization by incorporating all samples with confident inlier predictions, regardless of whether they are actually inliers or outliers. However, its pseudo-label accuracy remains low, which ultimately constrains overall performance. Since clients in OSSFL lack reliable ground-truth supervision, the models are highly susceptible to noisy pseudo-labels, leading to progressively worse pseudo-labels.

FedOpenMatch addresses these challenges by generating pseudo-labels with the global model and keeping them fixed during local training, thereby avoiding degradation of pseudo-label quality caused by unstable updates. Coupled with the proposed components, the data utilization rate steadily increases while maintaining relatively high pseudo-label accuracy. As a result, FedOpenMatch

432 achieves consistent state-of-the-art performance across nearly all settings, demonstrating both its
 433 robustness and superiority, particularly under challenging data configurations.
 434

435 4.3 ABLATION STUDIES

437 In this section, we evaluate the effectiveness of key components in FedOpenMatch, and examine its
 438 sensitivity to hyper-parameters. Due to space limit, we put the detailed results in Appendix A.2.

439 **Effect of gradient stop (GS).** We conduct experiments under CIFAR100@50@10@– configura-
 440 tions to investigate the effect of GS. As shown in Fig. 3 and Fig. 4 in Appendix A.2, with the
 441 adoption of GS, the performance is consistently improved, with the open-set accuracy gap reaching
 442 up to 10.68%. Meanwhile, we observe that the gradient similarity between the inlier classifier and
 443 OVA classifier branches is highly unstable. When their optimization directions happen to align, the
 444 two branches temporarily reinforce each other (e.g., in the early training stage without GS, the ac-
 445 curacy can exceed that with GS). However, as the gradient similarity drops, the branches interfere
 446 with each other and overall performance degrades. In other settings (e.g., Fig. 5 in Appendix A.2),
 447 where the similarity remains low throughout training, the performance without GS is consistently
 448 worse than with GS. Overall, GS is important for achieving stable and superior performance.

449 **Effect of logit adjustment.** To mitigate the imbalance between inliers and outliers in OVA training
 450 (Sec. 3.3), we introduce logit adjustment. We evaluate its effect on CIFAR-100@80@25@Dir(0.1)
 451 under different adjustment weights ω . As shown in Fig. 6 and in Fig. 7 in Appendix A.2, open-set
 452 accuracy drops significantly (18.19%) when $\omega = 0$, as the OVA classifier becomes biased toward the
 453 majority classes (unseen classes). Performance peaks when $\omega = 1$, validating the effectiveness of
 454 logit adjustment in correcting class imbalance.

455 **Effect of logit consistency regularization.** We propose a weak-strong logit consistency regulariza-
 456 tion to better exploit unlabeled samples (Sec. 3.4). We study the effect of the consistency weight λ
 457 on CIFAR-100, with results in Fig. 6 in Appendix A.2. Both closed-set and open-set accuracy are
 458 sensitive to λ . When $\lambda = 0$, closed-set and open-set accuracy drop by 4.82% and 5.61%, respec-
 459 tively, indicating the necessity of logit consistency. The best closed-set accuracy is achieved at $\lambda =$
 460 2 (improving 0.9% over $\lambda = 1$), but with a 4.7% drop in open-set accuracy. Overall, $\lambda = 1$ provides
 461 the best trade-off between closed-set and open-set performance.

462 We further compare our proposed logit consistency loss (Eq. (8)) with the probability consistency
 463 loss (Eq. (7)). As shown in Fig. 6 in Appendix A.2, our LCR loss significantly boosts both
 464 closed-set and open-set accuracy, for example, by 4.83% and 3.68% under data configuration CI-
 465 FAR100@80@25@Dir(0.1), demonstrating its superior ability to transfer richer information.

466 5 CONCLUSION

469 In this work, we formulate the practical yet underexplored problem of open-set semi-supervised
 470 federated learning, where the distributed unlabeled dataset contains samples from classes unseen in
 471 the labeled data. To address this challenge, we propose the first OSSFL framework, FedOpenMatch,
 472 which effectively leverages distributed open-set unlabeled data to improve model performance under
 473 both closed-set and open-set scenarios. We conduct extensive experiments on widely used bench-
 474 mark datasets, demonstrating that, despite its simplicity, FedOpenMatch outperforms existing ap-
 475 proaches by a clear margin, particularly under complex data configurations. We also provide detailed
 476 analyses to validate the contribution of each proposed component.

477 6 LIMITATION AND FUTURE WORK

480 While FedOpenMatch demonstrates significant empirical gains, a rigorous theoretical under-
 481 standing of its underlying mechanisms remains incomplete – an open challenge shared by many SSL
 482 approaches. We leave a more formal theoretical analysis to future work. In addition, several promis-
 483 ing extensions remain. For example, the inlier and OVA classifiers may complement each other
 484 when their optimization directions are aligned, suggesting the potential of adaptively controlling the
 485 gradient stop mechanism or explicitly promoting consistency between their optimization processes
 to further enhance overall performance.

486 REFERENCES
487

- 488 Sikai Bai, Shuaicheng Li, Weiming Zhuang, Jie Zhang, Kunlin Yang, Jun Hou, Shuai Yi, Shuai
489 Zhang, and Junyu Gao. Combating data imbalances in federated semi-supervised learning with
490 dual regulators. In *Proceedings of the AAAI Conference on Artificial Intelligence*, pp. 10989–
491 10997, 2024.
- 492 Baixu Chen, Junguang Jiang, Ximei Wang, Pengfei Wan, Jianmin Wang, and Mingsheng Long.
493 Debiased self-training for semi-supervised learning. *Advances in Neural Information Processing
494 Systems*, 35:32424–32437, 2022.
- 495 H Chen, R Tao, Yue Fan, Y Wang, M Savvides, J Wang, B Raj, X Xie, and Bernt Schiele. Softmatch:
496 Addressing the quantity-quality tradeoff in semi-supervised learning. In *Eleventh International
497 Conference on Learning Representations*, pp. 21. OpenReview. net, 2023.
- 498 Yanbei Chen, Xiatian Zhu, Wei Li, and Shaogang Gong. Semi-supervised learning under class
499 distribution mismatch. In *Proceedings of the AAAI conference on artificial intelligence*, pp. 3569–
500 3576, 2020.
- 501 Yae Jee Cho, Gauri Joshi, and Dimitrios Dimitriadis. Local or global: Selective knowledge assimila-
502 tion for federated learning with limited labels. In *Proceedings of the IEEE/CVF International
503 Conference on Computer Vision*, pp. 17087–17096, 2023.
- 504 Ekin D Cubuk, Barret Zoph, Jonathon Shlens, and Quoc V Le. Randaugment: Practical automated
505 data augmentation with a reduced search space. In *Proceedings of the IEEE/CVF conference on
506 computer vision and pattern recognition workshops*, pp. 702–703, 2020.
- 507 Enmao Diao, Jie Ding, and Vahid Tarokh. Semifl: Semi-supervised federated learning for unlabeled
508 clients with alternate training. *Advances in Neural Information Processing Systems*, 35:17871–
509 17884, 2022.
- 510 Mohab M Eid Kishawy, Mohamed T Abd El-Hafez, Retaj Yousri, and M Saeed Darweesh. Federated
511 learning system on autonomous vehicles for lane segmentation. *Scientific Reports*, 14(1):25029,
512 2024.
- 513 Yue Fan, Anna Kukleva, Dengxin Dai, and Bernt Schiele. Ssb: Simple but strong baseline for
514 boosting performance of open-set semi-supervised learning. In *Proceedings of the IEEE/CVF
515 international conference on computer vision*, pp. 16068–16078, 2023.
- 516 Lan-Zhe Guo, Zhen-Yu Zhang, Yuan Jiang, Yu-Feng Li, and Zhi-Hua Zhou. Safe deep semi-
517 supervised learning for unseen-class unlabeled data. In *International conference on machine
518 learning*, pp. 3897–3906. PMLR, 2020.
- 519 Jun-Yi Hang and Min-Ling Zhang. Binary decomposition: A problem transformation perspective for
520 open-set semi-supervised learning. In *Forty-first International Conference on Machine Learning*,
521 pp. 1–14, 2024.
- 522 Kaiming He, Xiangyu Zhang, Shaoqing Ren, and Jian Sun. Deep residual learning for image recog-
523 nition. In *Proceedings of the IEEE conference on computer vision and pattern recognition*, pp.
524 770–778, 2016.
- 525 Rundong He, Zhongyi Han, Xiankai Lu, and Yilong Yin. Safe-student for safe deep semi-supervised
526 learning with unseen-class unlabeled data. In *Proceedings of the IEEE/CVF conference on com-
527 puter vision and pattern recognition*, pp. 14585–14594, 2022.
- 528 Dan Hendrycks and Thomas Dietterich. Benchmarking neural network robustness to common cor-
529 ruptions and perturbations. *arXiv preprint arXiv:1903.12261*, 2019.
- 530 Junkai Huang, Chaowei Fang, Weikai Chen, Zhenhua Chai, Xiaolin Wei, Pengxu Wei, Liang Lin,
531 and Guanbin Li. Trash to treasure: Harvesting ood data with cross-modal matching for open-set
532 semi-supervised learning. In *Proceedings of the IEEE/CVF international conference on computer
533 vision*, pp. 8310–8319, 2021.

- 540 Zhuo Huang, Li Shen, Jun Yu, Bo Han, and Tongliang Liu. Flatmatch: Bridging labeled data and
 541 unlabeled data with cross-sharpness for semi-supervised learning. *Advances in neural information*
 542 *processing systems*, 36:18474–18494, 2023.
- 543
- 544 Wonyong Jeong, Jaehong Yoon, Eunho Yang, and Sung Ju Hwang. Federated semi-supervised
 545 learning with inter-client consistency & disjoint learning. In *International Conference on*
 546 *Learning Representations*, pp. 1–15, 2021. URL <https://openreview.net/forum?id=ce6CFXBh30h>.
- 547
- 548 Peter Kairouz, H Brendan McMahan, Brendan Avent, Aurélien Bellet, Mehdi Bennis, Arjun Nitin
 549 Bhagoji, Kallista Bonawitz, Zachary Charles, Graham Cormode, Rachel Cummings, et al. Ad-
 550 vances and open problems in federated learning. *Foundations and Trends® in Machine Learning*,
 551 14(1–2):1–210, 2021.
- 552
- 553 Taehyeon Kim, Eric Lin, Junu Lee, Christian Lau, and Vaikkunth Mugunthan. Navigating data
 554 heterogeneity in federated learning: A semi-supervised approach for object detection. In *Thirty-*
 555 *seventh Conference on Neural Information Processing Systems*, pp. 1–23, 2023.
- 556
- 557 Alex Krizhevsky, Geoffrey Hinton, et al. Learning multiple layers of features from tiny images,
 558 2009.
- 559
- 560 Dong-Hyun Lee et al. Pseudo-label: The simple and efficient semi-supervised learning method for
 561 deep neural networks. In *Workshop on challenges in representation learning, ICML*, volume 3,
 562 pp. 896. Atlanta, 2013.
- 563
- 564 Seungjoo Lee, Thanh-Long V Le, Jaemin Shin, and Sung-Ju Lee. fl^2 : Overcoming few labels
 565 in federated semi-supervised learning. *Advances in Neural Information Processing Systems*, 37:
 566 43693–43714, 2024.
- 567
- 568 Muyang Li, Runze Wu, Haoyu Liu, Jun Yu, Xun Yang, Bo Han, and Tongliang Liu. Instant: Semi-
 569 supervised learning with instance-dependent thresholds. *Advances in Neural Information Pro-*
 570 *cessing Systems*, 36:2922–2938, 2023a.
- 571
- 572 Zekun Li, Lei Qi, Yinghuan Shi, and Yang Gao. Iomatch: Simplifying open-set semi-supervised
 573 learning with joint inliers and outliers utilization. In *Proceedings of the IEEE/CVF International*
 574 *Conference on Computer Vision*, pp. 15870–15879, 2023b.
- 575
- 576 Xiaoxiao Liang, Yiqun Lin, Huazhu Fu, Lei Zhu, and Xiaomeng Li. Rscfed: Random sampling
 577 consensus federated semi-supervised learning. In *Proceedings of the IEEE/CVF Conference on*
 578 *Computer Vision and Pattern Recognition*, pp. 10154–10163, 2022.
- 579
- 580 Dongping Liao, Xitong Gao, Yabo Xu, and Cheng-Zhong Xu. Progressive distribution matching
 581 for federated semi-supervised learning. In *Proceedings of the AAAI Conference on Artificial*
 582 *Intelligence*, pp. 5191–5199, 2025.
- 583
- 584 Yuzhi Liu, Huisi Wu, and Jing Qin. Fedcd: Federated semi-supervised learning with class awareness
 585 balance via dual teachers. In *Proceedings of the AAAI Conference on Artificial Intelligence*, pp.
 586 3837–3845, 2024.
- 587
- 588 Brendan McMahan, Eider Moore, Daniel Ramage, Seth Hampson, and Blaise Aguera y Ar-
 589 cas. Communication-Efficient Learning of Deep Networks from Decentralized Data. In
 590 Aarti Singh and Jerry Zhu (eds.), *Proceedings of the 20th International Conference on Artifi-*
 591 *cial Intelligence and Statistics*, volume 54 of *Proceedings of Machine Learning Research*, pp.
 592 1273–1282. PMLR, 20–22 Apr 2017. URL <https://proceedings.mlr.press/v54/mcmahan17a.html>.
- 593
- 594 Aditya Krishna Menon, Sadeep Jayasumana, Ankit Singh Rawat, Himanshu Jain, Andreas Veit, and
 595 Sanjiv Kumar. Long-tail learning via logit adjustment. In *International Conference on Learning*
 596 *Representations*, 2021. URL <https://openreview.net/forum?id=37nvvqkCo5>.
- 597
- 598 Takeru Miyato, Shin-ichi Maeda, Masanori Koyama, and Shin Ishii. Virtual adversarial training: a
 599 regularization method for supervised and semi-supervised learning. *IEEE transactions on pattern*
 600 *analysis and machine intelligence*, 41(8):1979–1993, 2018.

- 594 Yuval Netzer, Tao Wang, Adam Coates, Alessandro Bissacco, Baolin Wu, Andrew Y Ng, et al.
 595 Reading digits in natural images with unsupervised feature learning. In *NIPS workshop on deep*
 596 *learning and unsupervised feature learning*, pp. 4. Granada, 2011.
- 597 Avital Oliver, Augustus Odena, Colin Raffel, Ekin D Cubuk, and Ian J Goodfellow. Realistic eval-
 598 uation of deep semi-supervised learning algorithms. In *Proceedings of the 32nd International*
 599 *Conference on Neural Information Processing Systems*, pp. 3239–3250, 2018.
- 600 Jae Hyeon Park, Joo Hyeon Jeon, Jae Yun Lee, Sangyeon Ahn, Min Hee Cha, Min Geol Kim, Hyeok
 601 Nam, and Sung In Cho. Dynamic pseudo labeling via gradient cutting for high-low entropy
 602 exploration. In *Proceedings of the Computer Vision and Pattern Recognition Conference*, pp.
 603 20602–20611, 2025.
- 604 Kuniaki Saito, Donghyun Kim, and Kate Saenko. Openmatch: Open-set semi-supervised learning
 605 with open-set consistency regularization. *Advances in Neural Information Processing Systems*,
 606 34:25956–25967, 2021.
- 607 Micah J Sheller, Brandon Edwards, G Anthony Reina, Jason Martin, Sarthak Pati, Aikaterini Kotrot-
 608 sou, Mikhail Milchenko, Weilin Xu, Daniel Marcus, Rivka R Colen, et al. Federated learning in
 609 medicine: facilitating multi-institutional collaborations without sharing patient data. *Scientific*
 610 *reports*, 10(1):12598, 2020.
- 611 Kihyuk Sohn, David Berthelot, Nicholas Carlini, Zizhao Zhang, Han Zhang, Colin A Raffel,
 612 Ekin Dogus Cubuk, Alexey Kurakin, and Chun-Liang Li. Fixmatch: Simplifying semi-supervised
 613 learning with consistency and confidence. *Advances in neural information processing systems*,
 614 33:596–608, 2020.
- 615 Yidong Wang, Hao Chen, Qiang Heng, Wenxin Hou, Yue Fan, Zhen Wu, Jindong Wang, Marios
 616 Savvides, Takahiro Shinohashi, Bhiksha Raj, et al. Freematch: Self-adaptive thresholding for semi-
 617 supervised learning. In *The Eleventh International Conference on Learning Representations*, pp.
 618 20, 2022.
- 619 Qizhe Xie, Zihang Dai, Eduard Hovy, Thang Luong, and Quoc Le. Unsupervised data augmentation
 620 for consistency training. *Advances in neural information processing systems*, 33:6256–6268,
 621 2020.
- 622 Chen Yang, Meilu Zhu, Yifan Liu, and Yixuan Yuan. Fedpd: Federated open set recognition with
 623 parameter disentanglement. In *Proceedings of the IEEE/CVF International Conference on Com-*
 624 *puter Vision*, pp. 4882–4891, 2023.
- 625 Mingzhao Yang, Shangchao Su, Bin Li, and Xiangyang Xue. Exploring one-shot semi-supervised
 626 federated learning with pre-trained diffusion models. In *Proceedings of the AAAI Conference on*
 627 *Artificial Intelligence*, pp. 16325–16333, 2024.
- 628 Qing Yu, Daiki Ikami, Go Irie, and Kiyoharu Aizawa. Multi-task curriculum framework for open-
 629 set semi-supervised learning. In *European conference on computer vision*, pp. 438–454. Springer,
 630 2020.
- 631 Bowen Zhang, Yidong Wang, Wenxin Hou, Hao Wu, Jindong Wang, Manabu Okumura, and
 632 Takahiro Shinohashi. Flexmatch: Boosting semi-supervised learning with curriculum pseudo la-
 633 beling. *Advances in Neural Information Processing Systems*, 34:18408–18419, 2021.
- 634 Chao Zhang, Fangzhao Wu, Jingwei Yi, Derong Xu, Yang Yu, Jindong Wang, Yidong Wang, Tong
 635 Xu, Xing Xie, and Enhong Chen. Non-iid always bad? semi-supervised heterogeneous federated
 636 learning with local knowledge enhancement. In *Proceedings of the 32nd ACM International*
 637 *Conference on Information and Knowledge Management*, pp. 3257–3267, 2023a.
- 638 Jie Zhang, Xiaosong Ma, Song Guo, and Wenchao Xu. Towards unbiased training in federated open-
 639 world semi-supervised learning. In Andreas Krause, Emma Brunskill, Kyunghyun Cho, Barbara
 640 Engelhardt, Sivan Sabato, and Jonathan Scarlett (eds.), *Proceedings of the 40th International*
 641 *Conference on Machine Learning*, volume 202 of *Proceedings of Machine Learning Research*,
 642 pp. 41498–41509. PMLR, 23–29 Jul 2023b. URL <https://proceedings.mlr.press/v202/zhang23af.html>.

648 Yonggang Zhang, Zhiqin Yang, Xinmei Tian, Nannan Wang, Tongliang Liu, and Bo Han. Robust
649 training of federated models with extremely label deficiency. In *The Twelfth International Con-*
650 *ference on Learning Representations*, pp. 1–22, 2024.

651 Meilu Zhu, Jing Liao, Jun Liu, and Yixuan Yuan. Fedoss: Federated open set recognition via inter-
652 client discrepancy and collaboration. *IEEE Transactions on Medical Imaging*, 43(1):190–202,
653 2023.

654

655

656

657

658

659

660

661

662

663

664

665

666

667

668

669

670

671

672

673

674

675

676

677

678

679

680

681

682

683

684

685

686

687

688

689

690

691

692

693

694

695

696

697

698

699

700

701

702 **A EXPERIMENTAL DETAILS**

703

704 **A.1 IMPLEMENTATION**

705

706 In our experiments, we employ ResNet-18 (He et al., 2016) as the backbone for all datasets and
 707 methods, with the classification head implemented as described in the original papers. The number
 708 of clients is set to 50 for CIFAR100@50@-@- and 100 for the other settings. In each communication
 709 round, 10 clients are randomly selected for local training. Following prior work, we assign equal
 710 weight to each local model for aggregation.

711 We train the models for 600 communication rounds and adopt SGD with a momentum of 0.9 and
 712 weight decay of 0.0005 as the optimizer. The learning rate is initialized at 0.03 and decayed using
 713 a cosine schedule. The number of local training epochs for clients and server are set to $E_c = 5$ and
 714 $E_s = 5$, respectively. For all methods, the client batch size is 32, and the server batch size is 10 or
 715 250 depending on whether the number of labeled samples is fewer or greater than 1000. Following
 716 prior work, we employ confidence thresholds $\tau_{in} = 0.95$ for inlier pseudo-labels, and $\tau_{pos} = 0.99$,
 717 $\tau_{neg} = 0.01$ for OVA pseudo-labels. The weight for logit adjustment is set to $\omega = 1$ and the weight
 718 of LCR (Eq. (8)) is set to $\lambda = 1$ across all settings.

719 **Fair Comparison.** To ensure a fair comparison, we implement the federated versions of the baseline
 720 OSSL algorithms following their official implementation and use the hyperparameters recommended
 721 in their respective papers. The data distribution is consistent across all methods. We conduct *three*
 722 *independent runs* on all datasets using random seeds (0, 10, and 100). After each communication
 723 round, we evaluate the global model on the original test set and report the mean and standard error
 724 of closed-set accuracy and open-set accuracy.

725 All experiments are conducted on an Ubuntu 16.04 server using PyTorch 1.8.0. The **source code**
 726 and detailed library dependencies are provided in Supplementary Material.

728 **A.2 DETAILED EXPERIMENTAL RESULTS.**

729

731 Due to the space limitation, we present the detailed experimental results here.

732 **Influence of local epochs.** To understand the influence of client local training epochs, we conduct
 733 additional experiments on CIFAR-100 dataset. As shown in Fig. 11, using too few local epochs leads
 734 to underfitting and slow convergence, requiring many more communication rounds to achieve rea-
 735 sonable performance. In contrast, using too many local epochs can improve accuracy but introduces
 736 the risk of unstable or divergent training due to excessive local drift. The conclusion is consistent
 737 with prior SSFL work (Diao et al., 2022).

738 **Influence of OVA threshold.** To understand the influence of OVA threshold, we conduct exper-
 739 iments on CIFAR-100 with varying OVA threshold. The results are presented in Fig. 12, which
 740 suggests that closed-set accuracy remains stable across a wide range of OVA thresholds, indicating
 741 that this component has limited impact on inlier classification. In contrast, open-set accuracy is
 742 more sensitive to the threshold value. A low threshold admits more samples during training but also
 743 introduces substantial noise, leading to unstable optimization and degraded open-set performance.
 744 Therefore, using a higher threshold is generally preferable, as it filters out unreliable samples and
 745 stabilizes training.

746 **Robustness to complex data settings.** To better simulate real-world data complexity, we construct
 747 a variant of CIFAR-100, denoted as CIFAR100-C, by applying diverse corruption types following
 748 the protocol of (Hendrycks & Dietterich, 2019)¹. In this dataset, 70% of the samples are corrupted
 749 to induce feature shift, while the remaining 30% are kept clean. Each client then samples its local
 750 data according to a Dirichlet distribution (consistent with our main experiments) to additionally
 751 introduce label shift. This setup reflects realistic scenarios where both feature shift and label shift
 752 coexist. Under these challenging conditions, FedOpenMatch still achieves the best performance by
 753 a clear margin as shown in Fig. 13, demonstrating strong robustness to complex and heterogeneous
 754 data distributions.

755 ¹We follow the official instructions at <https://github.com/hendrycks/robustness>.

756 **Comparison under scenarios with high unknown-class prevalence.** To further evaluate FedOpen-
 757 Match under scenarios where unseen prevalence is very high, we conduct experiments on CIFAR-
 758 100 dataset with only 20 seen classes and the remaining 80 classes are unknown. Figure 14 shows
 759 that FedOpenMatch significantly outperforms baselines, demonstrating its effectiveness when un-
 760 known classes dominate the data distribution.

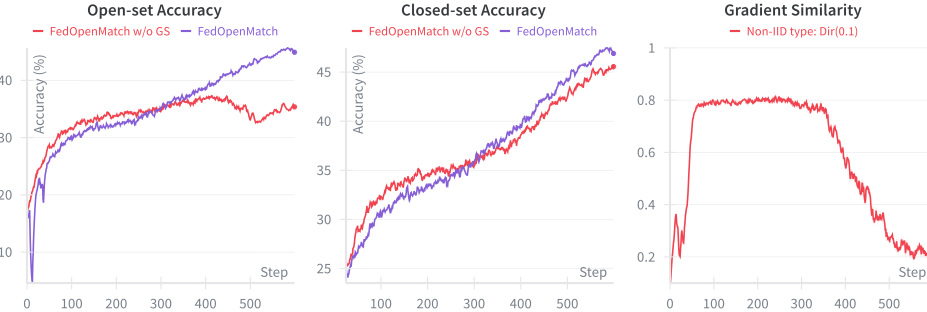
761 **Computation/communication overhead.** It is worth-noting that OVA classifier does not introduce
 762 much additional communication and computation overhead as it only consists of a two-layer projec-
 763 tion head and a linear classification head. The number of computation and communication overhead
 764 are negligible relative to the backbone.

765 **Comparison with different backbones.** To further assess the effectiveness and robustness of Fe-
 766 dOpenMatch across model architectures, we conduct additional experiments using WideResNet-
 767 28×2, a widely adopted backbone in the SSL and SSFL literature. As shown in Tab. 6, FedOpen-
 768 Match consistently achieves the best performance, demonstrating that its components do not rely on
 769 any backbone-specific assumptions.

770 **Ablation studies isolating each component.** In Sec. 4.3, we analyze the contribution of each indi-
 771 vidual component. Here, we provide additional experiments to further demonstrate the effectiveness
 772 and necessity of each component, as summarized in Tab. 7.

775 B THE USE OF LARGE LANGUAGE MODELS

777 During the preparation of this manuscript, we used ChatGPT to assist with writing by providing
 778 the prompt: “I am preparing a paper for submission to an international conference and would like
 779 your help to check for any grammatical issues and refine the wording or sentence structure where
 780 necessary to ensure conciseness and precision.” We applied its suggestions paragraph by paragraph,
 781 and all outputs were edited by us to ensure correctness.



793 Figure 3: Performance comparison of FedOpenMatch with and without the Gradient Stop (GS)
 794 strategy on CIFAR-100@50@10@Dir(0.1), along with the gradient similarity between the inlier
 795 classifier and OVA classifier branches. In the early training stage, the performance without GS
 796 surpasses that with GS, suggesting that the OVA classifier and inlier classifier can reinforce each
 797 other when their update directions are aligned. However, as training progresses, the gradients begin
 798 to diverge, and the resulting interference between the two classifiers leads to a performance drop.

799
 800
 801
 802
 803
 804
 805
 806
 807
 808
 809

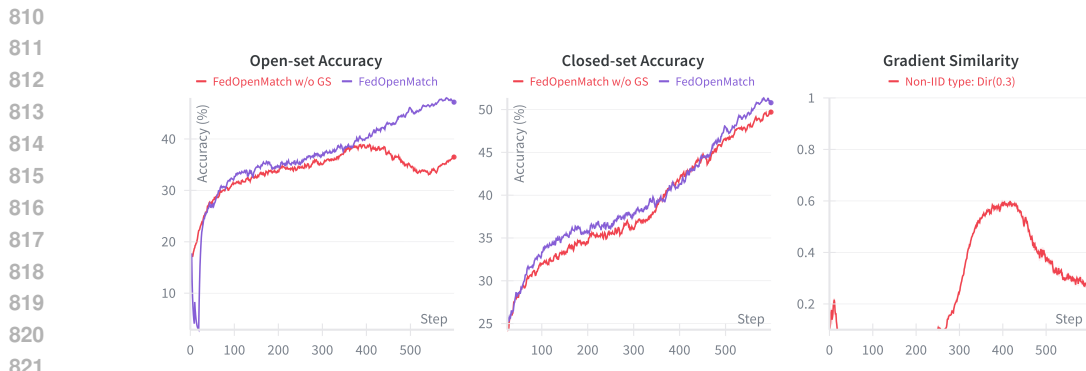
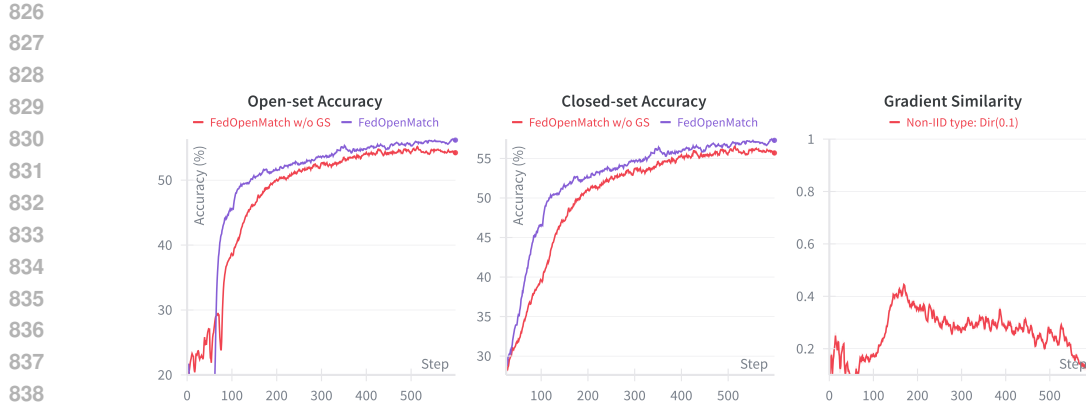
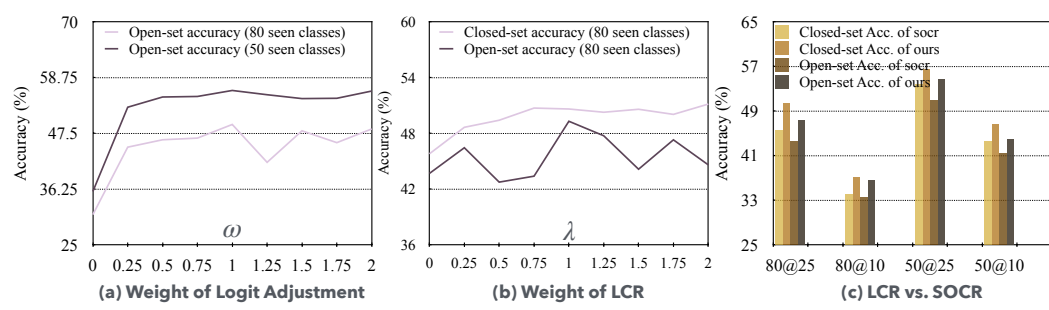


Figure 4: Performance comparison of FedOpenMatch with and without the Gradient Stop (GS) strategy on CIFAR-100@50@10@Dir(0.3), along with the gradient similarity between the inlier classifier and OVA classifier branches. Since the update directions diverge for most of the training process, the performance with GS surpasses that without GS, as expected.



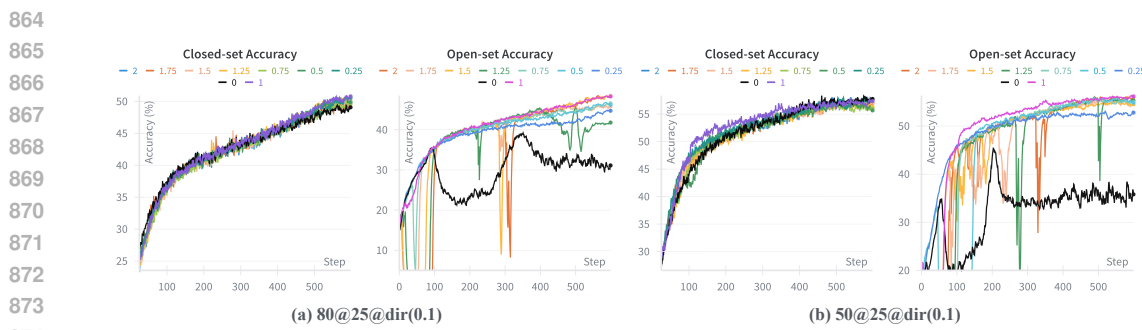
840
841
842
843
844
845
846

Figure 5: Performance comparison of FedOpenMatch with and without the Gradient Stop (GS) strategy on CIFAR-100@50@25@Dir(0.1), along with the gradient similarity between the inlier classifier and OVA classifier branches. The gradient similarity remains low throughout the training, thus the performance with GS consistently surpasses that without GS.



857
858
859
860
861
862
863

Figure 6: Ablation studies. For simplicity, we use X@Y to represents data setting with X seen classes and Y labeled samples per class. (a): FedOpenMatch with different ω under CIFAR-100@-@25@Dir(0.1) setting. Without logit adjustment ($\omega = 0$), the open-set accuracy degrades significantly. (b): FedOpenMatch with different λ under CIFAR-100@80@25@Dir(0.1) setting. The performance is improved with LCR loss. (c): Comparison of existing **SOCR** loss and our **LCR** loss under CIFAR100@-@-@Dir(0.1) setting. Our LCR outperforms existing SOCR across various settings.



875
876
877
878
879
880
881
882
883
884
885
886
887
888
889
890
891
892
893
894
895
896
897
898
899
900
901
902
903
904
905
906
907
908
909
910
911
912
913
914
915
916
917

Figure 7: Learning curves of training with various strength of logit adjustment (Eq. (6)) on CIFAR-100 dataset. The results present a clear accuracy margin between those with and without logit adjustment.

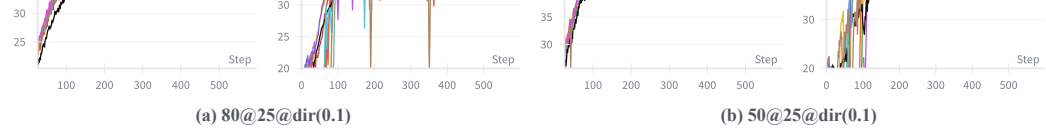


Figure 8: Learning curves of training with various weights of logit consistency regularization loss (Eq. (8)) on CIFAR-100 dataset. The performance gets clear improvement with logit consistency regularization loss.

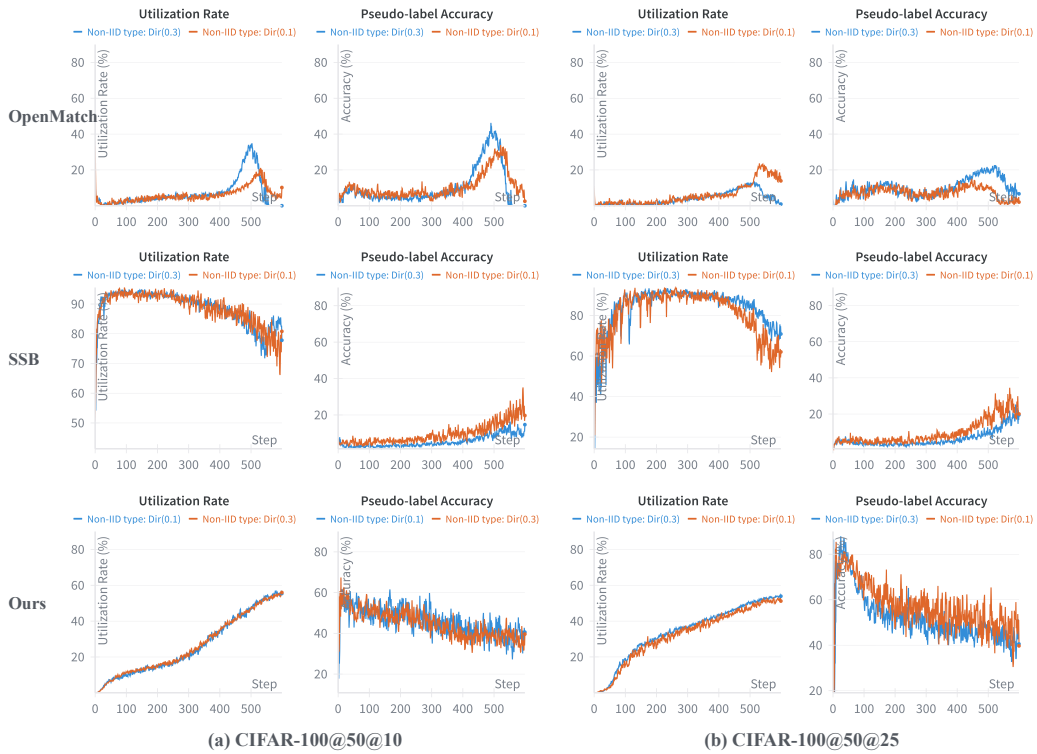
Table 6: Performance comparison of FedOpenMatch with state-of-the-art baselines using a different backbone (WideResNet-28×2). The results show that FedOpenMatch consistently achieves the best performance with a clear margin, demonstrating its robustness to different backbone architectures.

CIFAR-100	50@25@Dir(0.1) Open-set Acc	50@25@Dir(0.1) Closed-set Acc	80@25@Dir(0.1) Open-set Acc	80@25@Dir(0.1) Closed-set Acc
FedLabel	None	47.12	None	37.05
IOMatch	35.71	44.58	24.65	37.12
FedOpenMatch	50.16	52.14	42.69	43.23

Table 7: Ablation studies isolating each component. The results show the effectiveness and necessity of each module, confirming that each component contributes meaningfully to the overall performance of FedOpenMatch.

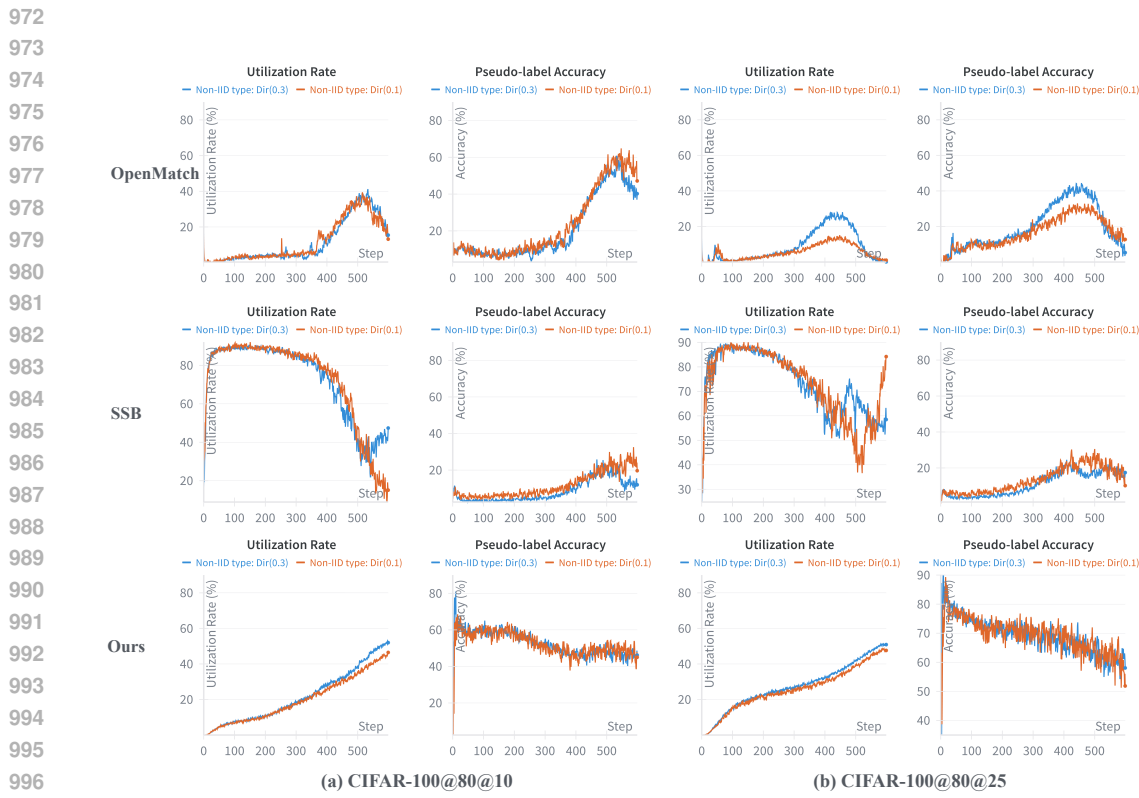
CIFAR100@80@25@Dir(0.1)	Base	Base+GS	Base + GS + LA	Base + GS + LA + LCR
Open-set Accuracy	34.81	39.51	43.65	48.36
Closed-set Accuracy	45.86	46.14	45.81	50.38

918
919
920
921
922
923
924
925
926
927
928
929



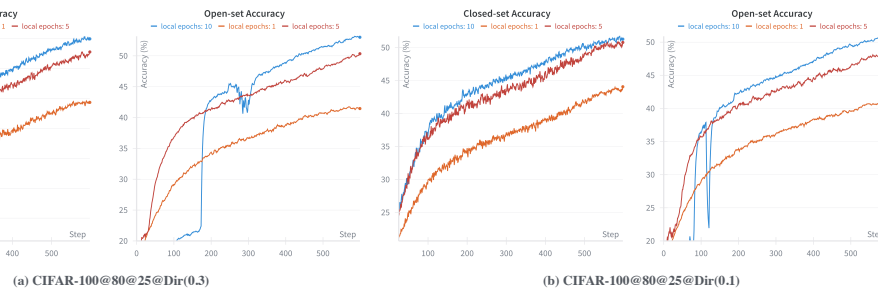
945
946
947
948
949
950
951
952
953
954
955
956
957
958
959
960
961
962
963
964
965
966
967
968
969
970
971

Figure 9: Comparison of **utilization rate** and **pseudo-label accuracy** of OpenMatch (Saito et al., 2021), SSB (Fan et al., 2023) and FedOpenMatch (ours), which share the same architecture. OpenMatch suffers from both a low data utilization rate and poor pseudo-label quality, as most samples are mistakenly identified as outliers by the imbalanced OVA classifier, thereby limiting its performance. SSB relaxes the pseudo-label filtering strategy to increase data utilization, but this introduces a large number of incorrect pseudo-labels. In contrast, FedOpenMatch addresses both issues simultaneously, achieving higher data utilization and more reliable pseudo-label accuracy.



998
999
1000
1001
1002
1003
1004
1005
1006
1007
1008
1009
1010
1011
1012
1013
1014
1015
1016
1017
1018
1019
1020
1021
1022
1023
1024
1025

Figure 10: Comparison of **utilization rate** and **pseudo-label accuracy** of OpenMatch (Saito et al., 2021), SSB (Fan et al., 2023) and FedOpenMatch (ours), which share the same architecture. OpenMatch suffers from both a low data utilization rate and poor pseudo-label quality, as most samples are mistakenly identified as outliers by the imbalanced OVA classifier, thereby limiting its performance. SSB relaxes the pseudo-label filtering strategy to increase data utilization, but this introduces a large number of incorrect pseudo-labels. In contrast, FedOpenMatch addresses both issues simultaneously, achieving higher data utilization and more reliable pseudo-label accuracy.



1018
1019
1020
1021
1022
1023
1024
1025

Figure 11: Performance comparison of FedOpenMatch with different numbers of local training epochs on the CIFAR-100 dataset. As shown, using too few local epochs leads to underfitting and slow convergence, requiring many more communication rounds to achieve reasonable performance. In contrast, using too many local epochs can improve accuracy but introduces the risk of unstable or divergent training due to excessive local drift. We adopt 5 local epochs in the main experiments, which provides a good balance—allowing clients to sufficiently learn from their local data while avoiding overfitting or instability.

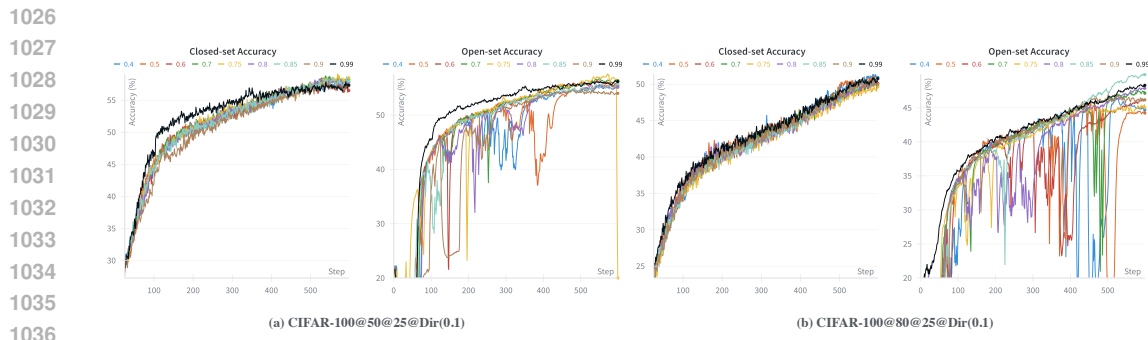


Figure 12: Performance comparison of FedOpenMatch under different OVA thresholds on the CIFAR-100 dataset. The results show that closed-set accuracy remains stable across a wide range of OVA thresholds, indicating that this component has limited impact on inlier classification. In contrast, open-set accuracy is more sensitive to the threshold value. A low threshold admits more samples during training but also introduces substantial noise, leading to unstable optimization and degraded open-set performance. Therefore, using a higher threshold is generally preferable, as it filters out unreliable samples and stabilizes training.



Figure 13: Performance comparison under complex settings where label shift and feature shift coexist. We further evaluate FedOpenMatch in a more realistic scenario that introduces both label shift and feature shift simultaneously. We compare against FedLabel and IOMatch, the two strongest-performing baselines. Across all metrics, FedOpenMatch maintains a clear performance margin over both methods, demonstrating its robustness and superiority under challenging, real-world data heterogeneity.

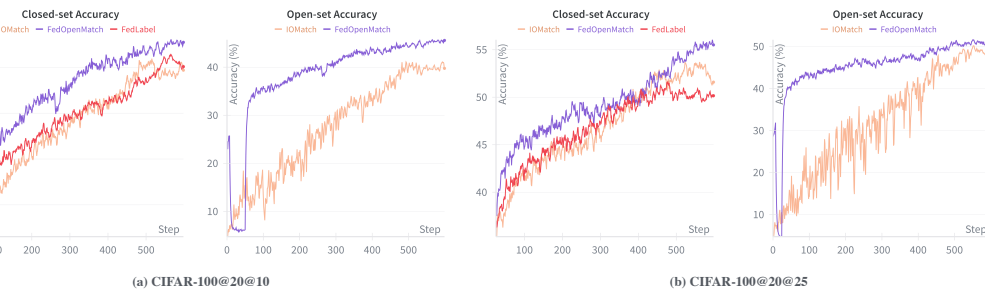


Figure 14: Performance comparison under extreme scenarios with high unknown-class prevalence. We further evaluate FedOpenMatch on CIFAR-100 with only 20 seen classes and 80 unseen classes, creating an extreme setting where unknown samples dominate the data. Even in this highly challenging scenario, FedOpenMatch consistently achieves the best performance among all methods, demonstrating strong robustness and clear superiority under extreme open-set conditions.

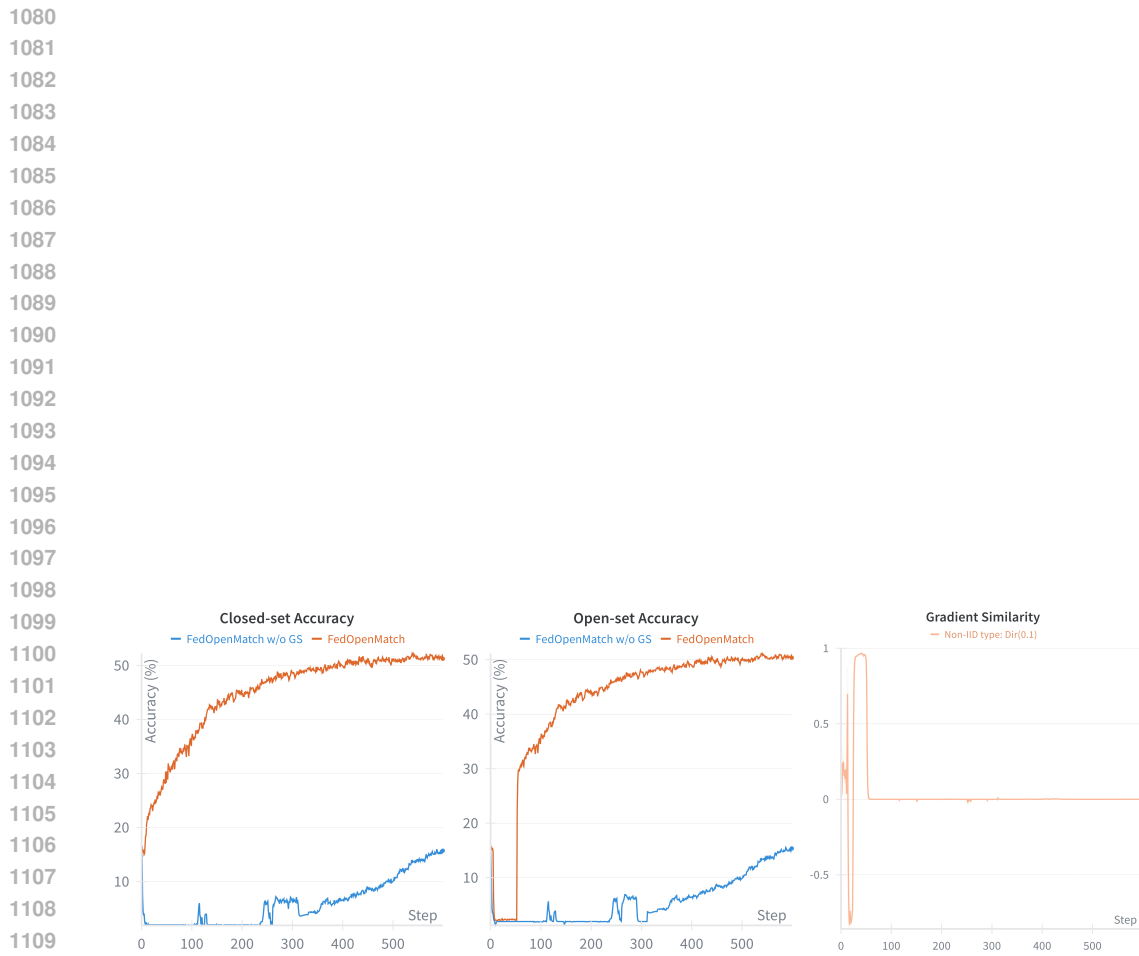


Figure 15: Performance comparison of FedOpenMatch with and without the Gradient Stop (GS) strategy on CIFAR-100@50@25@Dir(0,1) with different backbone (WideResNet-28x2), along with the gradient similarity between the inlier classifier and OVA classifier branches. The gradient similarity remains extremely low during the whole training process, which proves the clear performance gap between models with and without GS.

1116
1117
1118
1119
1120
1121
1122
1123
1124
1125
1126
1127
1128
1129
1130
1131
1132
1133